Development and characterization of novel cholangiocarcinoma cell sublines resistant to cisplatin or 5-fluorouracil

Kevin Delgado-Calvo[1,2] Oscar Briz[1,2], Candela Cives-Losada[3,4], Luke Boulter[5], Jose J.G. Marin[1,2], Elisa Lozano[1,2], Rocio I.R. Macias[1,2]
1) Experimental Hepatology and Drug Targeting (HEVEPHARM), Institute for Biomedical Research of Salamanca (IBSAL), University of Salamanca, Salamanca, Spain.
2) Center for the Study of Liver and Gastrointestinal Diseases (CIBEREHD), Carlos III National Institute of Health, Madrid, Spain.
3) Hepatobiliary Immunopathology Laboratory, IRCCS Humanitas Research Hospital, Rozzano, Milan, Italy.
4) Department of Health Sciences, University of Piemonte Orientale, Novara, Italy.
5) MRC-Human Genetics Unit, Institute of Genetics and Molecular Medicine, University of Edinburgh, Edinburgh, UK.

1. Background:

The efficacy of pharmacological treatment for cholangiocarcinoma (CCA) is very limited due to the presence of effective chemoresistance mechanisms. Therefore, there is an urgent need to improve therapeutic options, which requires the identification of new molecular targets. The development of novel 2D and 3D cellular models sensitive and resistant to chemotherapy enables progress in understanding the resistome and contributes to the search for new therapeutic tools. This study aims to generate and characterize the resistome of chemoresistant sublines derived from human CCA cells (EGI-1) resistant to cisplatin or 5-fluorouracil (5-FU), for their use in 2D and 3D cultures and the identification of new therapeutic targets.

2. Methods:

- Chemoresistant cells were generated by prolonged exposure to increasing concentrations of the drugs.
- Revertant cells were obtained by withdrawal of drug pressure.
- Cross-resistance was assessed by viability assays (MTT).
- Proliferation, migration, colony formation, and cell cycle distribution were analyzed using holographic microscopy and flow cytometry.
- Tumorigenic capacity was evaluated in immunodeficient athymic (*nu/nu*) mice.
- Resistome gene expression was determined by RNA-seq.
- Tumor-derived organoids were generated from xenograft tumors.

3. Results:

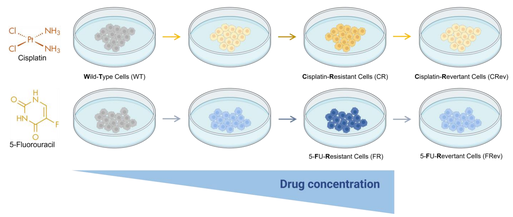

Figure 1. Schematic representation of the procedure used to generate EGI-1 cholangiocarcinoma cell lines resistant and revertant to cisplatin (CR and CRev) or 5-fluorouracil (FR and FRev) following 9 months of exposure to increasing concentrations of anticancer agents, and their subsequent complete withdrawal for 2 months. The initial concentrations used were 2 µM for cisplatin and 0.5 µM for 5-fluorouracil (5-FU), while the final concentrations reached were 9 µM for cisplatin and 10 µM for 5-fluorouracil. Arrows indicate successive culture passages with gradual increases in drug concentrations, as well as drug removal at the final stage. The figure was partially created with BioRender.com.

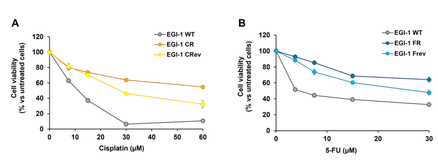

Figure 2. Concentration-dependent effect of cisplatin (A) and 5-FU (B) on cell viability, determined by the MTT-formazan assay after 72 h of exposure in EGI-1 WT cells and cells resistant or revertant to cisplatin (A) or 5-FU (B). Values represent the mean ± SEM of three independent experiments performed in triplicate. *, p < 0.01 compared with WT cells.

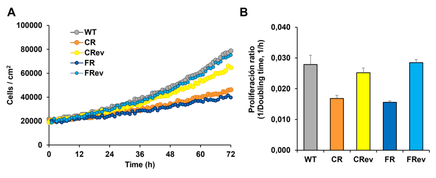

Figure 3. Representative recording of real-time proliferation of EGI-1 WT cells and cells resistant or revertant to cisplatin or 5-FU, monitored by holographic microscopy imaging (A). Images from 8 regions per well were acquired every 60 min for 72 h and analyzed using the corresponding software. Proliferation rate was calculated as the inverse of doubling time (B). Values represent the mean ± SEM of three independent experiments performed in duplicate. *, p < 0.01 compared with WT cells.

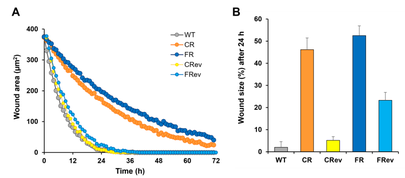

Figure 4. Representative recording of wound size progression over time in EGI-1 WT cells and cells resistant or revertant to cisplatin or 5-FU, monitored by holographic microscopy imaging (A). Images from 8 regions per well were acquired every 60 min for 72 h and analyzed using the corresponding software. Wound closure at 24 h was expressed as a percentage of the initial wound area (B). Values represent the mean ± SEM of three independent experiments performed in duplicate. *, p < 0.01 compared with WT cells.

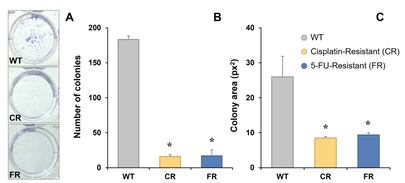

Figure 5. Representative images of colony formation in EGI-1 WT, cisplatin-resistant (CR), and 5-FU-resistant (FR) cells stained with crystal violet 7 days after seeding (A). Quantification of colony-forming units (B) and mean colony area (C). Results represent the mean ± SEM of three independent measurements. *, p < 0.05 compared with WT cells.

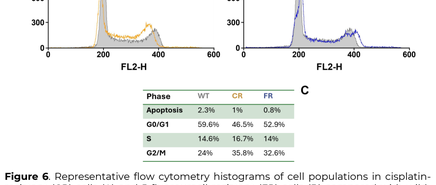

Phase	WT	CR	FR
Apoptosis	2.3%	1%	0.8%
G0/G1	59.6%	46.5%	52.9%
S	14.6%	16.7%	14%
G2/M	24%	35.8%	32.6%

Figure 6. Representative flow cytometry histograms of cell populations in cisplatin-resistant (CR) cells (A) and 5-fluorouracil-resistant (FR) cells (B) compared with wild-type EGI-1 (WT) cells. (C) Proportion of cells in each phase of the cell cycle (G0/G1, S, and G2/M), determined by DNA content based on propidium iodide (PI) staining intensity.

	IC_{50} Value				
Drug	EGI-1 WT	EGI-1 CR	RR	EGI-1 FR	RR
Cisplatin (µM)	12.9 ± 3.6	47.3 ± 3.2 [a]	3.7	9.3 ± 1.1	0.7
5-FU (µM)	11.0 ± 3.2	>30 [a]	>3	>30 [a]	>3
Gemcitabine (µM)	7.5 ± 3.4	12.0 ± 0.3	1.6	14.6 ± 1.5 [a]	1.9
Oxaliplatin (µM)	13.9 ± 2.5	24.5 ± 2.1 [a]	1.8	20.0 ± 0.1	1.4
Paclitaxel (nM)	7.7 ± 0.8	8.3 ± 1.1	1.1	12.1 ± 1.3	1.6
Irinotecan (µM)	4.5 ± 0.6	5.8 ± 1.1	1.3	44.9 ± 5.8 [a]	10
Bamet-UD2 (µM)	163 ± 22	262 ± 39	1.8	205 ± 42	1.4

Table 1. Drug concentrations required to inhibit 50% of cell growth (IC50) were calculated from dose–response curves using linear regression analysis. The degree of resistance of drug-resistant cells was determined as the resistance index (RR), defined as the ratio between the IC50 value of resistant cells and WT cells. NS, not significant.

Figure 7. In vivo tumor growth of wild-type EGI-1 (WT), cisplatin-resistant (CR), and 5-fluorouracil-resistant (FR) cells following subcutaneous injection of 10^6 cells into nude mice (A). Tumor weight at endpoint (day 18) (B). Values represent the mean ± SD of four tumors per group. *, p < 0.05 compared with tumors formed by WT cells.

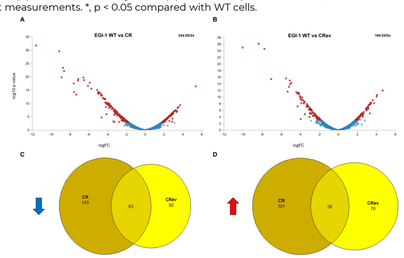

Figure 8. (A) Volcano plots of RNA-seq analysis comparing EGI-1 WT cells versus cisplatin-resistant (CR) cells. Each point represents a gene, showing expression change (logFoldChange) versus statistical significance (−$\log_{10}$ p-value). The total number of differentially expressed genes (DEGs) is indicated. (B) Volcano plot of RNA-seq analysis comparing EGI-1 WT cells versus cisplatin revertant (CRev) cells, with the number of DEGs indicated. (C) Venn diagram of downregulated differentially expressed genes. The left circle represents genes downregulated in WT vs CR, the right circle represents genes downregulated in WT vs CRev, and the intersection corresponds to genes common to both comparisons. (D) Venn diagram of upregulated differentially expressed genes, showing distribution between WT vs CR (left), WT vs CRev (right), and shared genes.

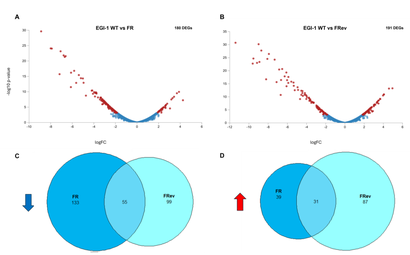

Figure 9. (A) Volcano plots of RNA-seq analysis comparing EGI-1 WT cells versus 5-FU-resistant (FR) cells. Each point represents a gene, showing expression change (logFoldChange) versus statistical significance (−$\log_{10}$ p-value). The total number of differentially expressed genes (DEGs) is indicated. (B) Volcano plot of RNA-seq analysis comparing EGI-1 WT cells versus 5-FU revertant (FRev) cells, with the number of DEGs indicated. (C) Venn diagram of downregulated differentially expressed genes. The left circle represents genes downregulated in WT vs FR, the right circle represents genes downregulated in WT vs FRev, and the intersection corresponds to genes common to both comparisons. (D) Venn diagram of upregulated differentially expressed genes, showing distribution between WT vs FR (left), WT vs FRev (right), and shared genes.

4. Conclusions

Two in vitro models of CCA cells in 2D and 3D cultures resistant to cisplatin or 5-FU have been developed and characterized. The partial reversibility of resistance after drug withdrawal suggests dynamic adaptive mechanisms. These models represent valuable tools for studying the resistome and for the preclinical evaluation of new therapeutic strategies in CCA.

BIBLIOGRAPHY

1. Marin JJG et al. Biochim Biophys Acta Mol Basis Dis. Apr; 1864(4 Pt B):1444-1453 (2018).
2. Boulter L et al. J Clin Invest. Mar 2;125(3):1269-85 (2015).
3. Perugorria MJ et al. Nat Rev Gastroenterol Hepatol. Feb;16(2):121-136. (2019).

Acknowledgements

This study was funded by the Instituto de Salud Carlos III (projects PI20/00189, PI22/00526, PI23/00681), co-funded by the European Union; the CIBERehd (CB06/04/0023); the Junta de Castilla y León (SA113P23); and the Fundación Científica AECC (Convocatoria de tumores raros 2023/2027), Spain. K.D-C. was supported by a predoctoral fellowship funded by the Junta de Castilla y León and the Fondo Social Europeo (ORDEN EDU/1868/2022) and by a "Beca Aprendizaje de Nuevas Tecnologías" funded by the AEEH (2025 Call).

Patient Friendly Lay Summary Panel

Aim:

CCA is difficult to treat because cancer cells often become resistant to chemotherapy drugs such as cisplatin and 5-fluorouracil over time. This study aimed to better understand how this resistance develops by creating laboratory models of cancer cells that no longer respond to these treatments and by identifying possible new targets for future therapies.

Methods:

We exposed human CCA cells to chemotherapy over a long period of time to make them resistant to treatment. We studied how these cells changed by looking at: how they survive and growth, how they move, how they divide and their ability to form new tumors.

We also studied what happened when the drugs were removed.

To better mimic real tumors, we created organoids, which are small 3D structures that behave like tumors in the body..

Results:

We successfully created cancer cells resistant to each drug.

Some resistant cells also became less sensitive to other drugs.

Resistant cells grew and moved more slowly but could still to form tumors.

When the drugs were removed, some cells partially returned to normal behavior.

Around 200 genes showed changes linked to resistance, and similar results were seen in the organoid models.

Conclusion:

The results suggest that resistance to chemotherapy may not be permanent and can change over time.

These new laboratory models will help researchers better understand resistance and may support the development of more effective treatments for patients in the future.